

OOMMF micromagnetic simulations of a square permalloy thin film

Giovanni Caligari, Matteo Venturelli

Abstract

The micromagnetic platform OOMMF was used to simulate the time evolution of a square thin film of permalloy ($\text{Ni}_{80}\text{Fe}_{20}$) at finite temperature. The minimum uniaxial anisotropy constant $K_1 = 330 \text{ kJ/m}^3$ which guaranteed an out-of-plane remanent magnetization (starting from an out-of-plane configuration of the magnetic moments) was found with a precision of 5kJ/m^3 . Upon implementing the Dzyaloshinskii–Moriya interaction in the simulations, the evolution of the sample starting from a two-domain configuration was studied. The value of the DMI constant D determined the speed and the extent of the domain wall propagation during the simulations. Finally, several ways to evaluate the anisotropic magnetoresistance of the formed domain walls were discussed.

Introduction

The project involves micromagnetic simulations of a permalloy sample ($\text{Ni}_{80}\text{Fe}_{20}$). Permalloy is a material notable for its very high magnetic permeability and significant anisotropic magnetoresistance. The sample consists of a square thin film (whose side length is $3 \mu\text{m}$ and whose thickness is 2 nm) near to the Spin Re-orientation Transition (SRT) condition. The SRT is a phenomenon which occurs in materials that have a strong easy-axis anisotropy and causes the change of the direction of the magnetic moments of the material at a specific temperature or applied magnetic field [10], thus the sample has to be evaluated at a finite T . The chosen temperature should be slightly below the one at which the transition takes place, that is between $T = 60 \text{ K}$ [11] and $T = 80 \text{ K}$ [12] for $\text{Ni}_{80}\text{Fe}_{20}$.

The project consists of three main requests. The first one is to determine the minimum uniaxial anisotropy constant K_1 such that the remanent magnetization is out-of-plane, starting from an initial condition in which the magnetization is out-of-plane.

The starting point for the second request is no more

a single domain: the sample is divided in two regions in which the magnetization is still out-of-plane, but with opposite orientation. Also, the Dzyaloshinskii–Moriya interaction (DMI) has to be taken into account. DMI is a type of magnetic interaction that arises from the combination of spin-orbit coupling and broken inversion symmetry in magnetic materials. This energy term can modify the evolution of the system, and the goal is to determine the relation between the strength of this interaction and the modification of the domain walls' structure.

The last request consists in the calculating the anisotropic magnetoresistance (AMR) of the domain walls as a function of the strength of the DMI. AMR is a property of a material which defines the variation of electrical resistance as a function of the direction of an applied magnetic field.

In order to distinguish between the two different out-of-plane magnetization orientations, a red-white-blue color scale is used in the simulations: the red regions indicate that the magnetic moments are oriented along $+z$, whereas the blue regions indicate a $-z$ orientation. The arrows describe the intensity and the direction of the magnetic moments in the xy plane.

First Request

First of all, the atlas and the cell size for the mesh were defined. The cell size should be set to be lower than the exchange length which, for the considered sample, is equal to:

$$l_{ex} = \sqrt{\frac{2A}{\mu_0 M_s^2}} \approx 4.292 \text{ nm}$$

The available computational power was not enough to be able to set a cell size lower than 4.292 nm , so a value of `cellsize = 6 nm` was chosen.

Then, Landau-Lifshitz-Gilbert (LLG) equation energy terms were specified: exchange energy (exchange coefficient $A = 6 \text{ pJ/m}$), uniaxial anisotropy (variable

crystalline anisotropy constant K_1 , direction $+z$) and demagnetizing energy were included. To implement thermal effects in the simulations, `UHH_ThetaEvolve` extension [4] was installed. `UHH_ThetaEvolve` has been developed based on `EulerEvolve` and introduces a highly irregular fluctuating field in the LLG equation to include the effect of temperature in the micromagnetic model [8]. Treating the thermal perturbations (which have a finite correlation time) as white noise is allowed only if the actual correlation time is much smaller than the response time of the system under study. These assumption may become wrong for low temperatures. Concerning the chosen timestep, which is not variable but fixed in this evolverclass, numerical stability has to be considered: if the timestep is set too big, the whole system will become unstable and will start to oscillate. A simulation with temperature set to zero (`UHH_ThetaEvolve` will use variable timesteps then) has to be run to check for the lower boundary of the timesteps in this run. Choosing a timestep well below this value should be safe. In order to establish the correct value for the `fixed_timestep` parameter, several simulations with different values of the anisotropy constant K_1 were carried out, which yielded a timestep of 2.5 ps.

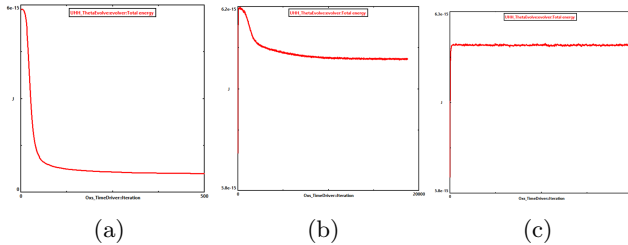


Figure 1: Graphs showing the total energy of the sample as a function of the iteration number for $K_1 = 0 \text{ kJ/m}^3$ (1a), $K_1 = 325 \text{ kJ/m}^3$ (1b) and $K_1 = 330 \text{ kJ/m}^3$ (1c). In all three cases the simulation was stopped once the energy reached a stationary value.

Simulations were run until an equilibrium configuration for the system was reached (i.e. until the total energy of the system stabilized to a constant value, as one can see from Figure 1).

Since the initial configuration of the sample (spins oriented out of plane along $+z$) is a local minima for the total energy of the system, a weak external field ($B = 1 \mu\text{T}$) was set for one iteration in order to break the symmetry and let the system evolve to a lower energy state. This procedure was necessary only in the $T = 0$ case (thermal excitations at $T > 0$ could break the initial symmetry).

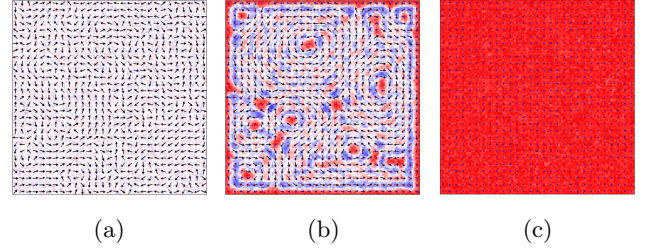


Figure 2: Top view of the equilibrium configurations of the sample magnetic moments for $K_1 = 0 \text{ kJ/m}^3$ (2a), $K_1 = 325 \text{ kJ/m}^3$ (2b) and $K_1 = 330 \text{ kJ/m}^3$ (2c). The configuration associated to $K_1 = 0 \text{ kJ/m}^3$ is almost perfectly in-plane, whereas for $K_1 = 330 \text{ kJ/m}^3$ the magnetic moments direction is perfectly out-of-plane. From the equilibrium condition associated to $K_1 = 325 \text{ kJ/m}^3$ one can notice that shape anisotropy and uniaxial anisotropy are almost balanced: the spins are neither totally in-plane nor out-of-plane.

If the uniaxial anisotropy term is not considered ($K_1 = 0$), the system evolves in such a way to align the spins to the xy plane (Figure 2a). This is due to the fact that the initial condition is associated to an high demagnetizing energy: the configuration of the magnetic moments produces a large region around the sample in which the demagnetizing field is not negligible. If the magnetic moments were parallel to the xy plane and layed in a closure domain structure instead, the demagnetizing energy would be sensibly lower. The effect of the uniaxial anisotropy energy term is to introduce an energy cost $E = K_1 \sin \vartheta^2$ when the magnetic moments are not aligned to the easy axis. This causes the moments to align to the easy axis, and higher K_1 values tend to emphasize this effect. As a matter of fact, the increase of the value of K_1 slows down the convergence to the in-plane solution until the cost of aligning the magnetic moments to the plane (in terms of anisotropy energy) overcomes the demagnetizing energy gain. Starting from $K_1 = 0$ and incrementing its value by 50 kJ/m^3 at a time, different simulations were performed to determine the range in which the behavior change took place. Further tests were carried out and the range was reduced up to 5 kJ : as one can observe from Figures 2b and 2c, this transition occurs between $K_1 = 325 \text{ kJ/m}^3$ (magnetic moments are mostly in-plane) and $K_1 = 330 \text{ kJ/m}^3$ (all magnetic moments point out-of-plane).

Second Request

In this second part the atlas has been divided into two different regions with opposite out-of-plane magnetization (the first one directed along $+z$ and the second one along $-z$). The simulation parameters were not changed, except for the out-of-plane anisotropy constant which was set to the value $K_1 = 330 \text{ kJ/m}^3$. This was done in order to maintain an out-of-plane magnetization for both domains and to let the evolution of the system (including the domain wall formation) depend mainly on the strength of the Dzyaloshinskii–Moriya interaction.

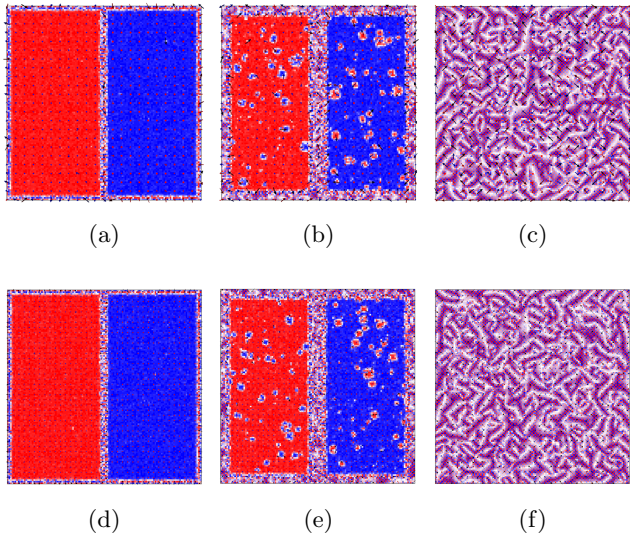


Figure 3: Top view of the configurations of the sample magnetic moments. The upper row images show the behavior of the sample for $D = -5 \text{ mJ/m}^2$ after 500 (3a), 1000 (3b) and 6000 (3c) iterations. The lower row images show the behavior of the sample for $D = +5 \text{ mJ/m}^2$ after the same number of iterations. Figures (3c) and (3f) show equilibrium configurations corresponding to a minima for the total energy. No evident differences can be spotted between the $D = -5 \text{ mJ/m}^2$ and the $D = +5 \text{ mJ/m}^2$ cases.

First of all, `Oxs_DMExchange6Ngbr` extension [5] was installed in order to implement DMI effects in the simulations. `TimeDriver` was used to observe the time evolution of the system. Because of the different framework, the procedure to establish the correct timestep for the simulation was performed again. As previously done, a simulation at zero temperature was run and the lower boundary of the timestep (in this case equal to 0.2 ps) was chosen as the `fixed_timestep` parameter. This timestep is one order of magnitude smaller with respect

to the one used for the first request, which means that the simulations now need approximately ten times the number of iterations in order to achieve the same total simulation time.

Simulations were initially performed with four different values of the DMI constant D (-5 mJ/m^2 , -0.5 mJ/m^2 , $+0.5 \text{ mJ/m}^2$ and $+5 \text{ mJ/m}^2$). The sign of the DMI constant determines the direction of the spin-orbit torque: if D is positive, the torque acts in a clockwise direction, while if D is negative, the torque acts in a counterclockwise direction. Simulations showed that, for our specific case study, the evolution of the system does not really depend on the sign of D , as it is possible to observe from Figure 3. The same behavior was observed for the cases in which the DMI is equal to -0.5 mJ/m^2 and $+0.5 \text{ mJ/m}^2$ (not shown).

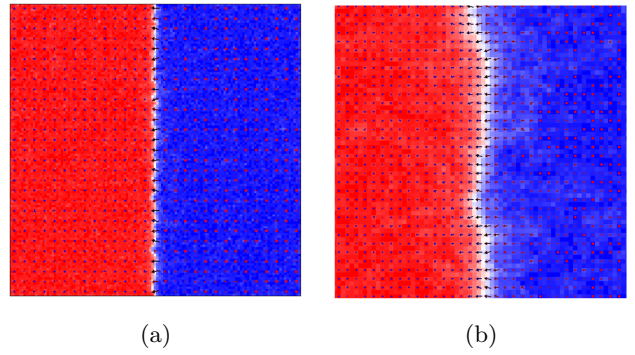


Figure 4: Top view of the configurations of the sample magnetic moments after 5000 iterations (1 ns) with $D = 0.5 \text{ mJ/m}^2$. (4a) shows the entire sample, which has no difference from the initial condition except for the domain wall formation. (4b) displays a $530 \text{ nm} \times 530 \text{ nm}$ detail of the domain wall, showing the characteristic magnetic moments rotation of a Néel wall.

In order to analyze the evolution of domain walls, the starting point is the case with the DMI constant equal to $+0.5 \text{ mJ/m}^2$. It is possible to observe from Figure 4 that a domain wall is formed between the two regions. As we can expect from literature [13], the formed wall is a Néel domain wall (the magnetization smoothly rotates across the domain wall and the rotation axis is parallel to the domain wall surface). At the end of the simulation (roughly after 7.5 ns) it can be observed that the domain wall surface expanded to generate a snake-like shape as shown in Figure 5.

Moving to the case in which $D = \pm 5 \text{ mJ/m}^2$, it is possible to highlight that the evolution of the domain wall is not only faster, but also more chaotic with respect to the case with smaller D . Small circular do-

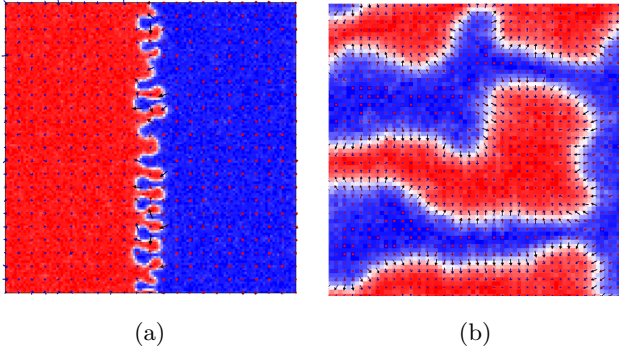


Figure 5: Top view of the configurations of the sample magnetic moments after 20000 iterations (4 ns) with $D = 0.5 \text{ mJ/m}^2$. (4a) shows the entire sample, whose domain wall exhibits a peculiar snake-like behavior. (4b) displays a $550 \text{ nm} \times 550 \text{ nm}$ detail of the domain wall, showing the characteristic magnetic moments rotation of a Néel wall.

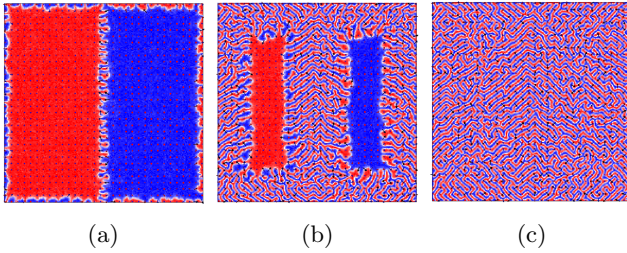


Figure 6: Top view of the configurations of the sample magnetic moments after 4400 (6a), 20000 (6b) and 38000 (6c) iterations with $D = 1 \text{ mJ/m}^2$. In this case the domain wall expands to the edges of the sample (6a) and slowly propagates towards the center of the two uniform magnetization domains until a stationary condition (6c) is reached.

mans started to grow up inside the uniform magnetization domains as can be seen in Figures 3b and 3e. The final stages of these simulations (Figures 3c and 3f) show that the initial separation between the two domains is completely lost and the system tends to maximize the domain walls surface.

In order to better understand the behaviour of the system, other simulations with intermediate values of the DMI constant were carried out. The results of the simulation run with $D = +1 \text{ mJ/m}^2$ are showed in Figure 6. One can observe a magnetization evolution which is similar to the previous cases, but more clear since it is less chaotic and it is faster in terms of number of iterations needed to reach convergence. During the

first iterations the domain wall is formed between the two regions, then it starts to form the snake-like shape seen before. In this case also the edges of the sample are affected by this behavior. As the simulation goes on, the system ends in a structure in which the region occupied by domain walls is maximized.

A possible explanation of this behavior could be that the addition of the Dzyaloshinskii–Moriya interaction has the effect of lowering the energy per unit volume related to the domain walls, since magnetic moments are not parallel in these regions and the DMI energy is then different from zero. Conversely, the initial condition in which all magnetic moments are parallel is associated to a DMI energy equal to zero. According to this assumptions, the DMI contribution drives the system towards a configuration in which the surface of the domain walls is maximized, since the DMI energy gain overcomes the exchange and uniaxial anisotropy energy costs.

Third Request

The starting point for the third request was the analysis of the previous situation, since not all the simulations led to the formation of a proper domain wall to which an anisotropic magnetoresistance could be associated. For this reason, the values of the DMI constant equal to $+5 \text{ mJ/m}^2$ and -5 mJ/m^2 have not been considered: the formation of domain walls was too disordered. Thus, the discussion is focused only on the results obtained with D value equal to $+0.5 \text{ mJ/m}^2$ and -0.5 mJ/m^2 .

As previously pointed out, the AMR is a property of a material which describes the dependence of electrical resistance on the angle between the direction of electric current and direction of the magnetization. A first issue arises from the fact that inside a domain wall the angle between the electric current and the direction of the magnetization is not constant, but it is a function of the spatial coordinate x . This means that the classical approach of injecting a current and measuring the resistance as a function the direction of the magnetization cannot be performed. Moreover, the team was not able to exploit OOMMF to perform this calculations since no extension developed for the 3D solver with this purpose was available. Several authors proposed different methods to deal with this problem:

- D. Buntinx et al. [19] used 2D solver in OOMMF to determine the equilibrium configuration of their sample and found the anisotropic magnetoresistance using another program;

- L.K. Bogart and D. Atkinson [15] used a method based on micromagnetic simulations in which the AMR for individual simulation cells is calculated, and then mapped the parameter space for different dimensions of their sample;
- M. Hayashi et al. [16] used an LLG micromagnetic simulator developed by M. R. Scheinfein;
- A. Manzin et al. [14] and Héctor Corte-Leon et al. used yet another micromagnetic solver for large-scale patterned media based on non-structured meshing [18].

Unfortunately, the installed extension to deal with temperature and Dzyaloshinskii–Moriya interaction work only with `Oxsii`, the OOMMF 3D solver, thus using the 2D solver was not an option.

A more "traditional" approach was then tried out in order to find an AMR value associated to the domain wall. However the definition of the AMR leads to the following expression:

$$AMR = \frac{\rho_{\parallel} - \rho_{\perp}}{\rho}$$

where ρ_{\parallel} is the longitudinal resistivity (case $\mathbf{J} \parallel \mathbf{M}$) and ρ_{\perp} is the transverse resistivity (case $\mathbf{J} \perp \mathbf{M}$). Since OOMMF does not provide a way to perform voltage measurements, the team did not have access to the values of the resistivity of the sample. So a step further could be the derivation of the resistivity both along the parallel and perpendicular direction starting from the scattering lenght of the electrons in the sample. Indeed, using the Drude model it is possible to obtain the following expression for the conductivity:

$$\sigma = \frac{ne^2\tau}{m^*}$$

but in order to exploit this formula, the relaxation time τ and the effective mass m^* of the electron are needed. Since τ is inversely proportional to the scattering lenght of the electrons, knowing the scattering lenght along both the perpendicular and parallel direction would provide the solution. These values, however, depend strongly not only on the material, but also on geometric factors and magnetic moments orientation. In order to estimate τ_{\parallel} and τ_{\perp} a lot of assumptions on the crystalline structure and the behavior of electrons in the system are required, leading to an unsubstantial result.

Another approach that was tried out to fulfill the request follows an AMR model provided by A. Manzin

et al. [14]. Starting from the application of an electric field it is possible to write local Ohm's law:

$$\mathbf{J} = \sigma \mathbf{E}$$

and since:

$$\mathbf{E} = -\nabla\phi$$

one obtains the following expression:

$$\nabla \cdot [\sigma(\mathbf{r}) \nabla \phi(\mathbf{r})] = 0$$

where:

$$\sigma(\mathbf{r}) = \sigma_0 [1 + \kappa \cos^2 \theta(\mathbf{r})]^{-1}$$

κ is the requested AMR value that would be calculated through numerical methods. The main issue with this approach, apart from the lack of informations on the values of numerical constant such as σ_0 , is the dependence of κ from the applied electric field \mathbf{E} which is not a given quantity. The result is indeed drastically affected by the choice of the electric field and for this reason it is impossible to determine κ without a strong assumption on \mathbf{E} that the team was not able to properly justify.

Due to all the discussed problems, the team was not able to determine the anisotropy magnetoresistance of the domain wall.

Conclusions

In the case of the first two requests, the initial considerations on the behavior of the system were verified by the simulations results. As a matter of fact, the increase in the uniaxial anisotropy parameter K_1 resulted in a switch from an in-plane configuration of the magnetic moments to a completely out-of-plane one, preserving the initial condition. The found value of K_1 at which the change of behavior takes place is $K_1 = 330 \text{ kJ/m}^3$, which is approximately three orders of magnitude higher with respect to the typical uniaxial anisotropy value for permalloy ($\approx 0.5 \text{ kJ/m}^3$). This means that in an experimental framework the magnetic moments would probably spontaneously align to the xy plane (shape anisotropy prevails over uniaxial anisotropy).

In the simulations run to fulfill the second request, the value of K_1 was set to $K_1 = 330 \text{ kJ/m}^3$ in order to maintain a spontaneous out-of-plane magnetization for the single domain configuration and DMI effects were introduced. In a real situation (low K_1 value) one would probably observe an in-plane configuration of the magnetic moments way before the formation of domain walls. Within the simulation context, with an extremely high value of the out-of-plane

anisotropy constant, the DMI becomes crucial for the formation, evolution, shape and even growth speed of the domain walls. The system spontaneously evolves towards a configuration in which the surface occupied by domain walls is maximized in order to minimize the total energy of the sample. This process is faster for higher value of DMI, but even with $D = +5$ mJ/m² or $D = -5$ mJ/m² the total simulation time was larger than 1 ns.

Concerning the last request, the calculation of the AMR could not be simulated by means of OOMMF, so other approaches have been tried out. An in-depth analysis of literature was performed, and several techniques to calculate the AMR were discussed. However, the methods that the team found in literature were not applicable to this specific case-study due to the lack of informations and data regarding the resistivity and other properties of the material, which revealed to be essential for this kind of calculations.

References

- [1] GitHub repository containing the code used for the simulations. URL: https://github.com/VenturelliMatteo/OOMMF_Permalloy_thin_film.
- [2] The Object Oriented MicroMagnetic Framework (OOMMF) project at ITL/NIST. URL: <https://math.nist.gov/oommf/>.
- [3] OOMMF User Guide for release 2.0 beta 0, 30 September 2022. URL: <https://math.nist.gov/oommf/doc/userguide20b0/userguide.pdf>.
- [4] UHH_ThetaEvolve extension module for the implementation of thermal effects in OOMMF. URL: http://www.nanoscience.de/group_r/stm-spstm/projects/temperature/download.shtml.
- [5] DMExchange6Ngbr extension module for Dzyaloshinsky-Moriya interaction implementation in OOMMF. URL: <https://math.nist.gov/oommf/contrib/oxsext/>.
- [6] OOMMF Tutorial Part II: OOMMF Basics. URL: https://math.nist.gov/oommf/oommf_tutorial/oommf_tutorial-20200526.pdf.
- [7] OOMMF Tutorial Part III: Advanced Simulations. URL: https://math.nist.gov/oommf/oommf_tutorial/oommf_tutorial-20200602.pdf.
- [8] Jose Luis Garcia-Palacios and Francisco J Lazaro. "Langevin-dynamics study of the dynamical properties of small magnetic particles". In: *Physical Review B* 58.22 (1998), p. 14937.
- [9] S Rohart and A Thiaville. "Skyrmion confinement in ultra-thin film nanostructures in the presence of Dzyaloshinskii-Moriya interaction". In: *Physical Review B* 88.18 (2013), p. 184422.
- [10] Konstantin P Belov et al. "Spin-reorientation transitions in rare-earth magnets". In: *Soviet Physics Uspekhi* 19.7 (1976), p. 574.
- [11] JF Sierra et al. "Interface and temperature dependent magnetic properties in permalloy thin films and tunnel junction structures". In: *Journal of Nanoscience and Nanotechnology* 11.9 (2011), pp. 7653–7664.
- [12] Carl E Patton and Charles H Wilts. "Temperature Dependence of the Ferromagnetic Resonance Linewidth in Thin Ni–Fe Films". In: *Journal of Applied Physics* 38.9 (1967), pp. 3537–3540.
- [13] T Trunk et al. "Domain wall structure in Permalloy films with decreasing thickness at the Bloch to Néel transition". In: *Journal of Applied Physics* 89.11 (2001), pp. 7606–7608.
- [14] Alessandra Manzin et al. "Modeling of anisotropic magnetoresistance properties of permalloy nanostructures". In: *IEEE transactions on magnetics* 50.4 (2014), pp. 1–4.
- [15] LK Bogart and D Atkinson. "Domain wall anisotropic magnetoresistance in planar nanowires". In: *Applied Physics Letters* 94.4 (2009), p. 042511.
- [16] M Hayashi et al. "Influence of current on field-driven domain wall motion in permalloy nanowires from time resolved measurements of anisotropic magnetoresistance". In: *Physical review letters* 96.19 (2006), p. 197207.
- [17] Héctor Corte-León et al. "Anisotropic magnetoresistance state space of permalloy nanowires with domain wall pinning geometry". In: *Scientific Reports* 4.1 (2014), pp. 1–10.
- [18] Alessandra Manzin and Oriano Bottauscio. "A micromagnetic solver for large-scale patterned media based on non-structured meshing". In: *IEEE transactions on magnetics* 48.11 (2012), pp. 2789–2792.
- [19] Dieter Buntinx, Alexander Volodin, and Chris Van Haesendonck. "Influence of local anisotropic magnetoresistance on the total magnetoresistance of mesoscopic NiFe rings". In: *Physical Review B* 70.22 (2004), p. 224405.
- [20] T McGuire and RL Potter. "Anisotropic magnetoresistance in ferromagnetic 3d alloys". In: *IEEE Transactions on Magnetics* 11.4 (1975), pp. 1018–1038.